Advanced Materials Research *Online: 2014-08-11*
ISSN: 1662-8985, Vol. 996, pp 82-87
doi:10.4028/www.scientific.net/AMR.996.82

Accounting for a distribution of morphologies and orientations on stresses analysis by X-ray and neutron diffraction: Normalized Self-Consistent modeling

Viwanou HOUNKPATI[1,a *], Sylvain FREOUR[1,b], David GLOAGUEN[1,c] and Vincent LEGRAND[1,d]

[1]Université de Nantes, Centrale Nantes, Institut de Recherche en Génie Civil et Mécanique (UMR CNRS 6183), Equipe Etat Mécanique et Microstructure, 58 rue Michel Ange, BP 420, 44606, Saint-Nazaire cedex, France

[a]viwanou.hounkpati@univ-nantes.fr, [b]sylvain.freour@univ-nantes.fr, [c]david.gloaguen@univ-nantes.fr, [d]vincent.legrand@univ-nantes.fr

Keywords: Normalized self-consistent model, multiphase materials, morphologic texture, geometric orientation, residual stress, diffraction.

Abstract. The historical Eshelby-Kröner self-consistent model is only valid in the case when grains can be assumed similar to ellipsoids aligned preferentially along a same direction into the polycrystal. In this work, distributions of crystallites morphologies and geometrical orientations were accounted for, owing to the so-called normalized self-consistent model, in order to satisfy Hill's averages principles. Different nonlinear $\varepsilon_{\varphi\psi}$-vs.-$\sin^2\psi$ distributions were predicted in elasticity, even in the absence of crystallographic texture, in the case when several morphologies and geometrical orientations coexist within the same polycrystal.

Introduction

Polycrystals with a morphological texture have macroscopic anisotropic properties in the absence of crystallographic texture. Many studies have been conducted to characterize the mechanical properties of such materials. The classical Eshelby-Kröner self-consistent model enables to take into account non-spherical grains when certain conditions are fulfilled [1-3]. According to these restrictions, only an ideal morphological texture can be taken into account through (identical) ellipsoidal inclusions whose principal axes are aligned along specific directions in the specimen. Such a microstructure is not generally observed in a real specimen; several morphologies or several grains with different morphological orientations could coexist within the same crystalline material. It is the case, for example, of titanium alloy Ti-17 polycrystal which consists of needle-shaped α crystallites mixed to slightly equiaxed prior β-grains [4]. Another example could be chosen among composite materials, made of epoxy resin and carbon-epoxy reinforcing strips, exhibiting an in-plane distribution on the morphologies [5], the microstructure of which was successfully modeled through disc-shaped inclusions.It was recently numerically shown [5] that in such a situation, the Eshelby-Kröner self-consistent model does not simultaneously fulfil anymore both the so-called "Hill's average relations over the mechanical states", historically established in [6]. Therefore, this theoretical approach fails to represent a morphological texture featuring various grain shapes or a relative disorientation of the morphologies coexisting. The main interest of the present contribution is to show the possible influence of this morphological texture in the context of stress analysis by diffraction, in elasticity, using a normalized elastic self-consistent model. Then, we will be interested in the $\varepsilon_{\varphi\psi}$-vs.-$\sin^2\psi$ diagrams.

If transversely isotropic grains are randomly oriented, the effective property of the polycrystal will be approximately isotropic, with values depending on the volume fraction and aspect ratio of the inclusions [7]. A random morphologic texture can then be neglected without consequence, within the context of modelling the multi-scale behaviour of heterogeneous materials consisting of quasi-isotropic elementary inclusions. This was demonstrated, at least numerically in [4]. Therefore, specimens investigated here were assumed to be made of two or three preferential morphological orientations.

X-ray diffraction probes Coherently Diffracting Domains (CDD) that are smaller than or equal to grain size In this work, we admit that the mechanical state of CDD and the mechanical state of the grain/crystal that contains it are equal.

Normalized self-consistent modeling

It was shown by Li [8] that all micromechanical approaches should (i) provide a diagonally symmetric stiffness tensor, (ii) give identical thermal stress tensors using two equivalent methods, (iii) satisfy the internal-consistency relationships between the effective moduli, and (iv) exhibit the correct behaviors at dilute and (v) unitary concentration limits. Unfortunately, the application of traditional scale transition models such as Mori-Tanaka or Eshelby-Kröner self-consistent models to the case of multi-phase materials containing heterogeneities of different shapes does not simultaneously satisfy all these five fundamental criteria. It often occurs that the first three criteria are not fulfilled [5,9].

To overcome all these several theoretical difficulties, Li [8] proposed an effective-medium-field micromechanics approximation using normalized strain localization tensor. Under this approximation, the strain localization tensor ${}_{Ri}A^{i}$ can be written, in the grains frame of reference Ri attached to its main axes (in a given phase i), as:

$${}_{Ri}A^{i}(\Omega) = {}_{Ri}T^{i}(\Omega) : \left\langle {}_{Ri}T^{i}(\Omega) \right\rangle^{-1} \tag{1}$$

where Ω describes the crystalline orientations within a polycrystalline sample through the three Eulerian angles φ_1, ϕ and φ_2 [10]; $\langle\ \rangle$ stands for the volume average over the whole polycrystal; A:B denotes the double scalar product using the Einstein summation convention; ${}_{Ri}T^{i}$ is the strain localization tensor in the Eshelby-Kröner self-consistent approach, written in Ri:

$${}_{Ri}T^{i}(\Omega) = \left[I + {}_{Ri}E : \left({}_{Ri}c^{i}(\Omega) - {}_{Ri}C \right) \right]^{-1} \tag{2}$$

where ${}_{Ri}c^{i}$ and ${}_{Ri}C$ are respectively the mesoscopic and the macroscopic stiffness tensors in Ri coordinate system; I represents the fourth order identity tensor. ${}_{Ri}E$ is the Morris tensor, expressed in the grains coordinate system Ri, which represents the interaction between an inclusion with a given morphology and the Homogeneous Equivalent Medium [10]:

$${}_{Ri}E_{ijkl} = \frac{1}{4\pi} \int_0^{\pi} \sin\theta d\theta \int_0^{2\pi} \gamma_{ikjl} d\phi = {}_{Ri}S^{Esh}_{ijkl} \, {}_{Ri}C^{-1}_{ijkl} \tag{3}$$

$$\text{with } \gamma_{ikjl} = K^{-1}_{ik}(\xi)\xi_j\xi_l,\ K_{jp}(\xi) = {}_{Ri}C_{ijpl}\xi_i\xi_l,\ \xi_1 = \frac{\sin\theta\cos\phi}{a_1},\ \xi_2 = \frac{\sin\theta\sin\phi}{a_2} \text{ and } \xi_3 = \frac{\cos\theta}{a_3} \tag{4}$$

where ${}_{Ri}S^{Esh}$ is the Eshelby tensor; the coefficients a_i are the lengths of the principal axes of the ellipsoid, used to describe grains shape. To account for various grain morphologies or geometrical orientations within the same polycrystal, the Morris tensor ${}_{Ri}E$ does not keep the general isotropic form commonly used, because new nonzero terms appear in ${}_{Ri}C$ and must be taken into account in the calculation of Morris tensor. All the components of Morris tensor were taken into account in this work. The local strain (at the i-phase grain scale) ε^{IIi} can then be obtained by:

$$\varepsilon^{IIi}(\Omega) = {}_{RI}A^{i}(\Omega) : \varepsilon^{I} = {}_{RI}T^{i}(\Omega) : \left\langle {}_{RI}T^{i}(\Omega) \right\rangle^{-1} : \varepsilon^{I} \tag{5}$$

where ε^I is the average macroscopic strain experienced by the polycrystal. The homogenization relation enabling to find the macroscopic stiffness ${}_{RI}C$ and the pseudo-macroscopic one ${}_{RI}C^i$ of a given phase i, in the macroscopic or polycrystal coordinate system RI, are respectively:

$$ {}_{RI}C = \left\langle {}_{RI}c^i(\Omega) :_{RI} A^i(\Omega) \right\rangle = \left\langle {}_{RI}c^i(\Omega) :_{RI} T^i(\Omega) \right\rangle : \left\langle {}_{RI}T^i(\Omega) \right\rangle^{-1} \tag{6} $$

$$ {}_{RI}C^i = \left\langle {}_{RI}c^i(\Omega) :_{RI} A^i(\Omega) \right\rangle_i : \left\langle {}_{RI}A^i(\Omega) \right\rangle_i^{-1} = \left\langle {}_{RI}c^i(\Omega) :_{RI} T^i(\Omega) \right\rangle_i : \left\langle {}_{RI}T^i(\Omega) \right\rangle_i^{-1} \tag{7} $$

$\langle\ \rangle_i$ stands for the volume average over the phase i. The transition between the local coordinate system (a_1, a_2, a_3) of the grain and the sample system (S_1, S_2, S_3) is made by the three Eulerian angles (see Fig. 1) in the Bunge convention [11,12] where the transformation matrix is given by:

$$ m(\varphi_1, \phi, \varphi_2) = \begin{bmatrix} \cos\varphi_1\cos\varphi_2 - \sin\varphi_1\sin\varphi_2\cos\phi & \sin\varphi_1\cos\varphi_2 + \cos\varphi_1\sin\varphi_2\cos\phi & \sin\varphi_2\sin\phi \\ -\cos\varphi_1\sin\varphi_2 - \sin\varphi_1\cos\varphi_2\cos\phi & -\sin\varphi_1\sin\varphi_2 + \cos\varphi_1\cos\varphi_2\cos\phi & \cos\varphi_2\sin\phi \\ \sin\varphi_1\sin\phi & -\cos\varphi_1\sin\phi & \cos\phi \end{bmatrix} \tag{8} $$

This matrix is applied, for a given rank four tensor K, as follows:

$$ {}_{RI}K_{ijkl} = m_{im}\, m_{jn}\, m_{ko}\, m_{lp}\ {}_{Ri}K_{mnop} \tag{9} $$

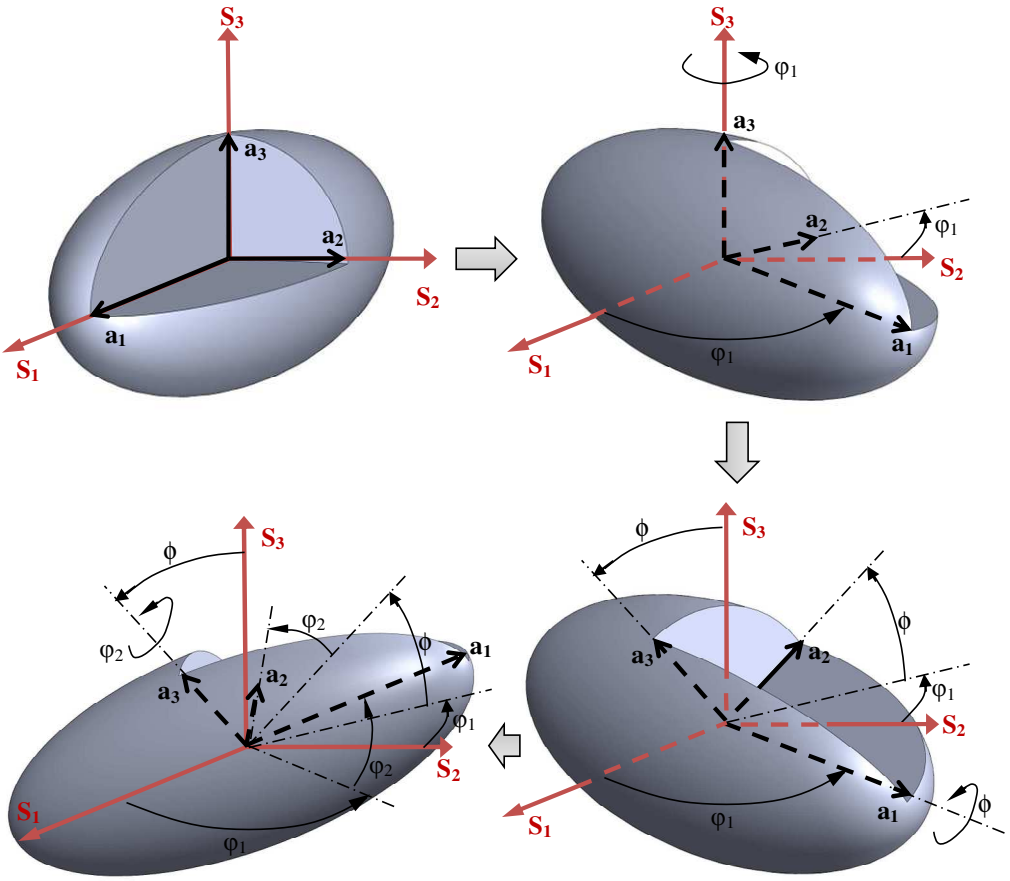

Figure 1 : Definition of the three Eulerian angles

Application of the normalized self-consistent model to stress analysis by diffraction methods

Diffraction methods like the well-known "$\sin^2\psi$ method" [12], used for determining internal stresses and elastic properties of polycrystalline materials, are based on the measurement of lattice spacings of the (hkl) planes in the crystallites contained in the diffracting volume. The diffraction geometry is shown in Fig. 2. The direction of the diffraction vector $n(\varphi,\psi) = (\sin\varphi\cos\psi, \sin\varphi\sin\psi, \cos\psi)$, is usually identified by the inclination φ and azimuthal ψ angles.

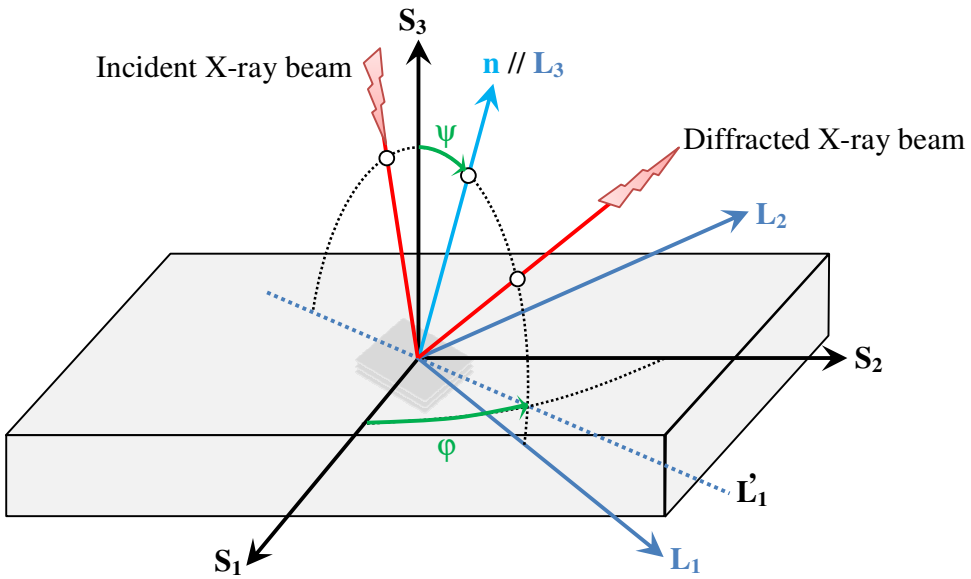

Figure 2 : The diffraction geometry

The lattice strain $\varepsilon^i_{\varphi\psi}$ measured by diffraction methods can be obtained as the average of the second order lattice strains over the i-phase diffracting grains for the considered (hkl) plane in the n direction. Using the normalized self-consistent model, $\varepsilon^i_{\varphi\psi}$ is given by the relation:

$$\varepsilon^i_{\varphi\psi} = \left\langle \varepsilon^{IIi}(\varphi,\psi,hkl)\right\rangle_{V_d} = n(\varphi,\psi).\left\langle \varepsilon^{IIi}(\Omega)\right\rangle_{V_d}.{}^t n(\varphi,\psi) = n(\varphi,\psi).\left\langle {}_{RI}T^i(\Omega)\right\rangle_{V_d} : \left\langle {}_{RI}T^i(\Omega)\right\rangle^{-1} : \varepsilon^I .{}^t n(\varphi,\psi) \quad (10)$$

where ${}^t n$ is the transpose of n and V_d stands for the diffracting volume (in i-phase).

Influence on $\varepsilon_{\varphi\psi}$-vs.-$\sin^2\psi$ distributions

The normalized self-consistent model described above is used to account for the influence of various distributions of crystallites morphologies and geometrical orientations in the context of predicting the lattice strains that would be measured owing to diffraction methods. From uniaxial tensile tests with σ^I_{11} = 100 MPa, $\varepsilon_{\varphi\psi}$-vs.-$\sin^2\psi$ curves have been simulated using Eq. 10. We described the morphology of the crystallites by a shape parameter denoted η, which is defined as the ratio of the principal axis of the ellipsoid (a_1) and the secondary axes (a_2 or a_3) of the ellipsoid ($\eta = a_1/a_2 = a_1/a_3$). η values chosen in this work are 1, 100 and 0.01 for spherical grains, fiber- and disc-shaped inclusions, respectively. An isotropic crystallographic texture was used by considering 10000 grains with random crystallographic orientations in each phase, to highlight the influence only of the morphological texture. Two-phase materials Al-SiC and Zn-Cd were investigated in this paper in order to show the influence of the crystal symmetry (cubic or hexagonal); Al-phase and Zn-phase were studied and assumed consisting of two preferential morphological orientations (arbitrarily chosen) in equal proportion. The three-dimensional orientation is described by the Eulerian angles defined in Fig. 1, using the transformation matrix $m(\varphi_1,\phi,\varphi_2)$. The others phases (SiC and Cd) are represented by a single morphology. Thus, by considering the three different

morphologies, the whole two-phases polycrystals were considered as a three-phases material. Fig. 3 shows $\varepsilon_{\varphi\psi}$-vs.-$\sin^2\psi$ diagrams for the (400) and (220) planes of Al-phase, and the (10.0) and (30.2) planes of Zn-phase, both representing 25% of volume fraction.

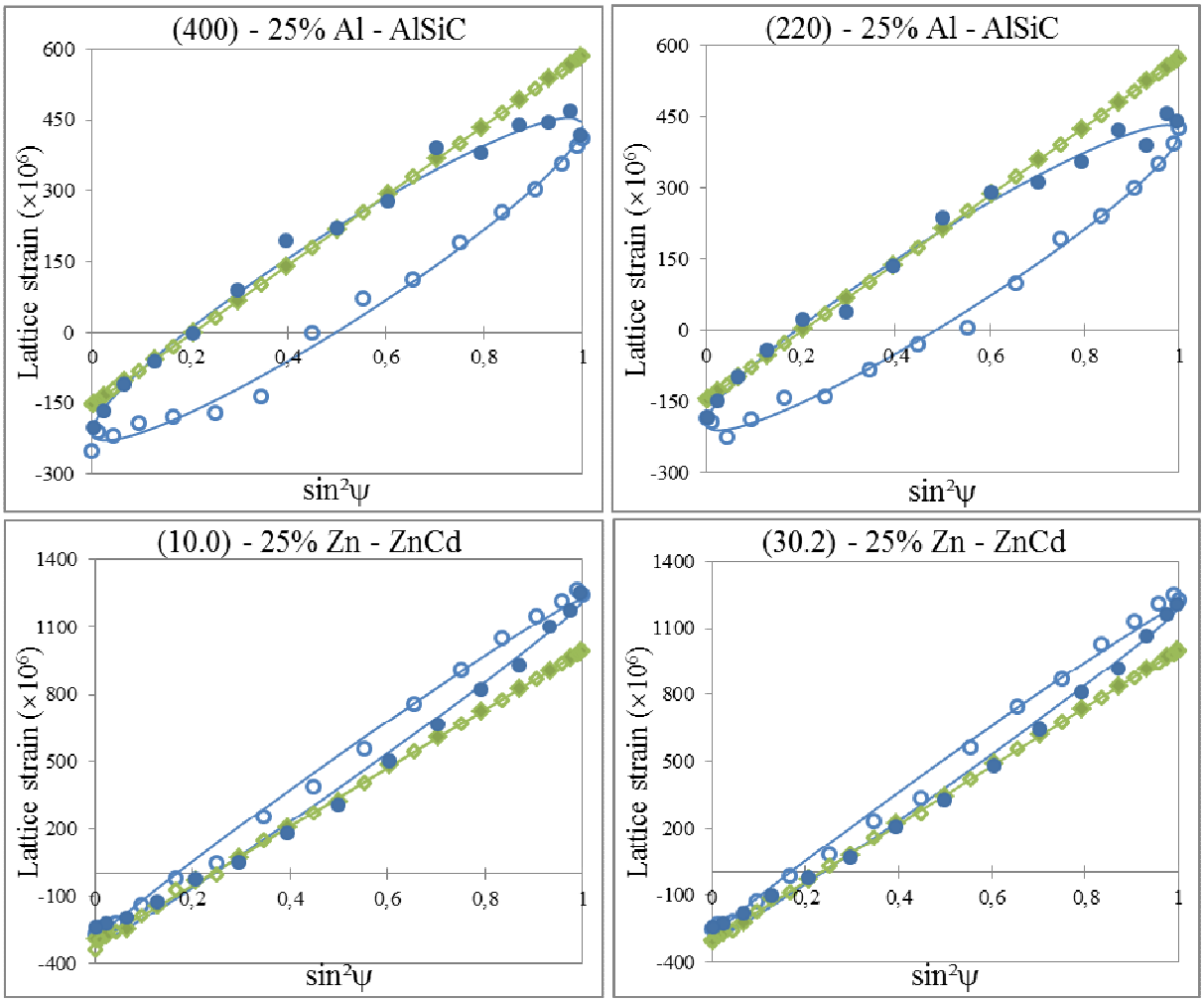

(a) Al or Zn: disc texture, m(0°, 0°, 0°) and m(90°, 20°, 270°) – SiC or Cd: fiber texture : m(0°, 0°, 0°)

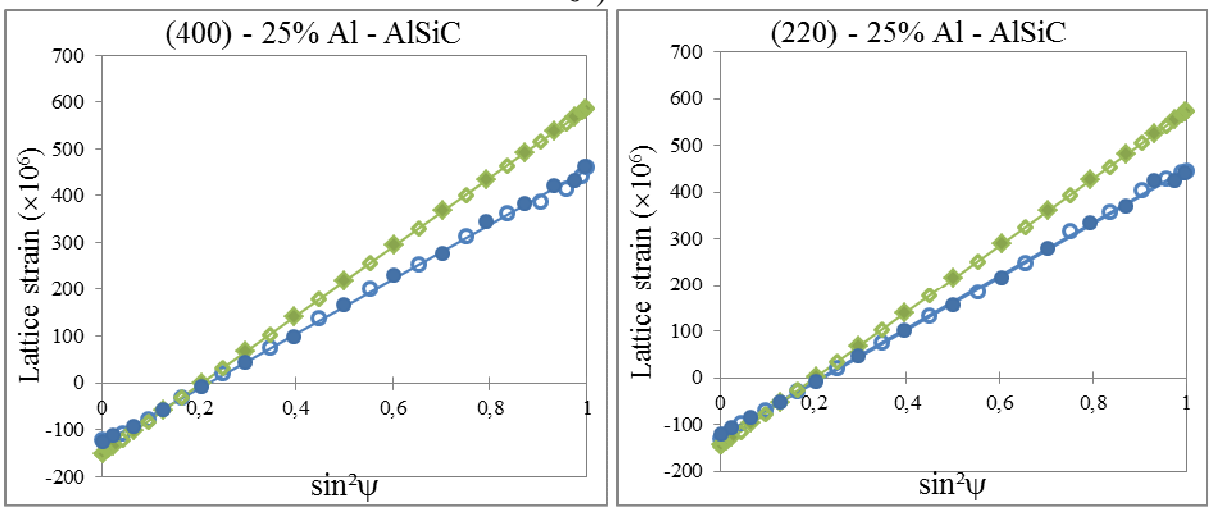

(b) Al: fiber texture, m(15°, 0°, 20°) and m(340°, 5°, 15°) – SiC: spherical grains

Figure 3 : Influence of distributions of crystallites morphologies and geometrical orientations on $\varepsilon_{\varphi\psi}$-vs.-$\sin^2\psi$ diagrams: (o) $\psi > 0$, (●) $\psi < 0$, (—) $A\sin^2\psi + B\sin2\psi + C$ regression; non-textured isotropic case with spherical grains: (◊) $\psi > 0$, (♦) $\psi < 0$, (—) $A\sin^2\psi + B\sin2\psi + C$ regression.

In the case of fiber texture, the transformation matrix m(0°, 0°, 0°) indicates a preferential alignment of the fibers along the loading direction S_1. In the case of disc texture m(0°, 0°, 0°) stands for the case when all the discs are contained in the sample surface S_1-S_2.

We note that the anisotropy introduced by the distribution of crystallites morphologies and geometrical orientations has greatly changed the $\varepsilon_{\varphi\psi}$-vs.-$\sin^2\psi$ distributions. As a result, more or less marked oscillations were observed, even in the absence of crystallographic texture. In the case of disc-shaped crystallites (Fig. 3a), $\varepsilon_{\varphi\psi}$ plotted versus $\sin^2\psi$ are almost elliptical instead of the straight line expected for the untextured material. Such a result obtained experimentally would have classically been attributed to the presence of a shear stress. In the case of fiber-shaped crystallites (example of Al-SiC in Fig. 3b), an almost straight line is obtained but its slope is different from the one corresponding to the isotropic case: this would certainly have led the experimenter to underestimate the magnitude of the actual stress state experienced by the polycrystal.

Conclusion

There exist four basic $\varepsilon_{\varphi\psi}$-vs.-$\sin^2\psi$ distributions [12]: (i) linear dependence obtained on quasi isotropic materials, (ii) ψ-splitting in the case of shear stress components, (iii) curved lines due to stress gradients or plastic deformation and finally (iv) oscillations associated with mechanical anisotropy (crystallographic texture). In this work, a micromechanical model was proposed to account for distributions of crystallites morphologies and geometrical orientations owing to the normalized self-consistent model in order to respect the diagonal symmetry of the stiffness tensor and to satisfy the internal-consistency relationships between the effective moduli. ψ-splitting curves were obtained in elasticity even in the absence of shear stress component or crystallographic texture.

References

[1] J. Krier, H. Ruppersberg, M. Berveiller, and P. Lipinski, Textures and Microstructures, 14-18 (1991), 1147-1152.

[2] B.C. Hendrix and L. G. Yu, Acta Materiala, 46 (1998), 127-135.

[3] N. Koch, U. Welzel, H. Wern and E. J. Mittemeijer, Philosophical Magazine, 84 (2004), 3547-3570.

[4] S. Fréour, E. Lacoste, F. Manuel and R. Guillén, Materials Science Forum, 681 (2011), 97-102.

[5] E. Lacoste, S. Fréour, and F. Jacquemin, Mechanics of Materials, 42 (2010), 218-226.

[6] R. Hill, Journal of the Mechanics and Physics of Solids, 15 (1967), 79-95.

[7] Y.P. Qiu and G.J. Weng, Mechanics of Materials, 12 (1991), 1-15.

[8] J. Y. Li, Mechanics of Materials, 31 (1999), 149-159.

[9] Y. Benveniste, G. J. Dvorak and T. Chen, Journal of the Mechanics and Physics of Solids, 39 (1991), 927-946.

[10] U. F. Kocks, C. N. Tomé and H. R. Wenk, Texture and Anisotropy, Cambridge University Press edition, 1998.

[11] H. J. Bunge, Texture analysis in materials science, Butterworth's edition, London, 1982.

[12] V. Hauk, Structural and Residual Stress Analysis by Nondestructive Methods, Elsevier Science edition, 1997.